Resonance Raman and Absorption Spectroscopy of the Lowest Triplet State of 1,3,5-Hexatriene and Deuteriated Derivatives at 183 K: Molecular Structure in the T_1 State

Frans W. Langkilde,*

Department of Physical Chemistry A, Royal Danish School of Pharmacy, 2 Universitetsparken, DK-2100 Copenhagen, Denmark

Robert Wilbrandt, Søren Møller,

Department of Environmental Science and Technology, Risø National Laboratory, DK-4000 Roskilde, Denmark

Albert M. Brouwer,

Laboratory of Organic Chemistry, University of Amsterdam, NL-1018 WS Amsterdam, The Netherlands

Fabrizia Negri, and Giorgio Orlandi*

Dipartimento di Chimica G. Ciamician, University of Bologna, I-40126 Bologna, Italy
(Received: December 28, 1990)

Time-resolved resonance Raman (RR) spectra of the lowest excited triplet state T_1 of (*E*)-1,3,5-hexatriene, (*E*)-3-deuterio-1,3,5-hexatriene, and (*E*)-1,1-dideuterio-1,3,5-hexatriene are obtained at 183 K. The T_1 potential energy surface (PES), determining energy minima, equilibrium geometries, frequencies, and normal modes of vibration, is calculated, and RR intensities are obtained on the basis of the Franck–Condon mechanism. By comparison with the calculated spectra, the observed RR spectra are assigned to an equilibrium mixture of planar *E* and *Z* species in the T_1 state. The relative intensity of the *E* and *Z* bands at temperatures between 293 and 183 K gives an upper limit of 0.22 kcal/mol for the energy difference between the planar *E* and *Z* forms. Time-resolved triplet–triplet absorption measurements as a function of temperature between 296 and 183 K yield a frequency factor *A* of 1.6×10^7 s^{-1} and an apparent activation energy E_a of 0.7 kcal/mol for the decay of the T_1 state. Consequently, an upper limit of 0.7 kcal/mol above the planar *E* and *Z* geometries is established for the possible local energy minimum at the twisted geometry. On the basis of these data, a PES is proposed for the T_1 state of 1,3,5-hexatriene with respect to torsion around the central CC bond and the C_2C_3 and C_4C_5 bonds.

I. Introduction

1,3,5-Hexatriene is an important model in studies of the photochemistry and photophysics of polyenes. The sensitized photoisomerization of 1,3,5-hexatriene (HT) proceeds through the lowest excited triplet state, T_1. In a recent paper we compared the T_1 resonance Raman (RR) spectra of (*E*)-1,3,5-hexatriene (EHT) and (*Z*)-1,3,5-hexatriene (ZHT),[1] and in another one we discussed quantum chemical calculations of T_1 absorption and RR spectra and compared the theoretical results with experimental T_1 RR spectra from d_0- and d_2-hexatrienes: EHT, (*E*)-3,4-dideuterio-1,3,5-hexatriene ((*E*)-HT-*3,4-d*$_2$), and (*E*)-2,5-dideuterio-1,3,5-hexatriene ((*E*)-HT-*2,5-d*$_2$).[2] We have also investigated various methylated derivatives of HT (ref 3, and references therein). All measurements were performed at room temperature in solution.

We found that the T_1 RR spectra of EHT and ZHT were identical, which we interpreted in terms of equilibration along the torsional coordinate of the central CC bond on the T_1 potential energy surface (PES) during the lifetime of T_1.[1] Furthermore, from the comparison of experimental and theoretical results,[2] we concluded that for HT two relative minima at planar *E* and *Z* geometries on the T_1 PES exist, and that both forms contribute to the RR spectrum, the *E* form being predominant and hence of lowest energy. While no evidence was found of the presence of a perpendicular form, twisted by 90° at the central CC bond, a *substantial* population of this form could not be excluded.

CHART I

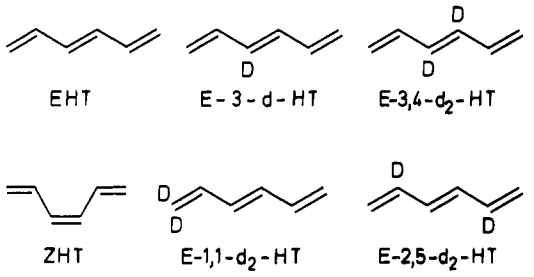

In the present paper, the study of T_1 HT is further pursued in two ways: (i) by recording of T_1 RR spectra at lower temperature and (ii) by investigation of additional deuteriated derivatives.

Several effects of lowering the temperature can be envisaged: (i) As the temperature is lowered, and the viscosity of the solution increases, diffusional processes, such as triplet energy transfer from the sensitizer to HT, and from HT to possible impurities, will be slowed down, thus influencing the kinetics of the buildup and possibly the decay of T_1 HT. (ii) With increasing viscosity, friction may become more important for the dynamics of the species in the T_1 state. (iii) The temperature will affect the rates of interconversion between the species corresponding to different minima on the T_1 PES and may influence the relative populations. When equilibration along the torsional coordinate is no longer possible, different spectra will be observed from solutions containing either the *E* or the *Z* ground-state isomer. If equilibration prevails, changes in the populations of the species present will be reflected in their contribution to the observed spectra. (iv) A narrowing of the population distributions at low temperature is expected to give rise to narrower Raman lines, improving resolution

(1) Langkilde, F. W.; Jensen, N.-H.; Wilbrandt, R. *J. Phys. Chem.* **1987**, *91*, 1040.
(2) Negri, F.; Orlandi, G.; Brouwer, A. M.; Langkilde, F. W.; Wilbrandt, R. *J. Chem. Phys.* **1989**, *90*, 5944.
(3) Langkilde, F. W.; Jensen, N.-H.; Wilbrandt, R.; Brouwer, A. M.; Jacobs, H. J. C. *J. Phys. Chem.* **1987**, *91*, 1029.

0022-3654/91/2095-6884$02.50/0

and sensitivity. (v) The lifetime of the triplet species, which may be affected by temperature in different ways, is observable from time-resolved RR or optical absorption measurements.

Investigation of additional deuteriated derivatives of (*E*)-1,3,5-hexatriene may provide a further test for the correlation between observed and calculated T_1 RR spectra. In particular, asymmetrical deuterium substitution increases the number of symmetry-allowed Raman bands of T_1 1,3,5-hexatriene. We have recently published a study of the Raman and infrared spectra of ground-state EHT, (*E*)-HT-*3,4-d*$_2$, (*E*)-3-deuterio-1,3,5-hexatriene ((*E*)-HT-*3-d*), (*E*)-1,1-dideuterio-1,3,5-hexatriene ((*E*)-HT-*1,1-d*$_2$), and (*E*)-HT-*2,5-d*$_2$, in order to improve the force field of (*E*)-1,3,5-hexatriene in the ground state.[4]

In the present paper, we report the time-resolved RR spectra of the lowest triplet state T_1 of EHT, ZHT, (*E*)-HT-*3-d*, and (*E*)-HT-*1,1-d*$_2$, obtained in solution at 183 K. Using a modified version of the semiempirical quantum mechanical consistent force field program (QCFF/PI),[5,6] calculations are performed on the T_1 state of the deuteriated compounds in the planar *E*, planar *Z*, and perpendicular or twisted (Tw) geometries. The structure of the T_1 state of 1,3,5-hexatriene is discussed by comparison of the experimental and theoretical results. In addition, we report time-resolved UV absorption measurements of the T_1 state of EHT as a function of temperature (296–183 K).

II. Experimental Methods

A. Materials. Acetonitrile-d_3 (Fluka, puriss., >99.8% D), cyclopentane (Fluka, for UV spectroscopy), methanol (Merck, p.a.), and acetone (Merck, p.a.) were used as received. 1,3,5-Hexatriene was obtained from Aldrich as a mixture of the *E* and *Z* isomers. The separation of the isomers has been described in detail previously.[1,7] The synthesis of (*E*)-HT-*3-d* and (*E*)-HT-*1,1-d*$_2$ has been described before.[4] Capillary gas chromatography (BP1 or DB225 columns, 50 °C, He carrier gas) showed (*E*)-1,3,5-hexatriene to be 99.4% pure (0.6% (*Z*)-1,3,5-hexatriene), (*Z*)-1,3,5-hexatriene 99.3% pure, (*E*)-HT-*3-d* 98% pure, and (*E*)-HT-*1,1-d*$_2$ 96% pure. ^{1}H NMR spectrometry (Bruker WM250, 250 MHz) of the deuteriated products indicated a high deuterium content (>95%).

The purified samples were distilled into glass capillaries under reduced pressure. The capillaries were cooled briefly, sealed, and kept in a freezer. Throughout the experiments, the capillaries with trienes were opened and solutions prepared and transferred to sample cells under an Ar atmosphere. Prior to the addition of triene, the solvents were purged with Ar for more than 35 min.

B. Raman Measurements. The experimental procedures for the time-resolved RR experiments have been described previously.[1,3] The triplet state of 1,3,5-hexatriene was produced by exciting acetone as sensitizer with a pump pulse (308 nm, ca. 5 mJ per pulse at the sample) from an excimer laser (Lambda Physics EMG 102E). The RR spectrum of 1,3,5-hexatriene in the T_1 state was obtained by using the second harmonic from a Nd:YAG-pumped dye laser (Quantel) as probe pulse (315 nm, ca. 2 mJ per pulse at the sample). Both lasers were pulsed at 5 Hz with pulse lengths of 10–15 ns, pump–probe time delays ranging from 60 to 1080 ns.

The detection system has been described in detail before.[3] Scattered Raman light was dispersed in a single-grating spectrometer (f = 600 mm, 2400 grooves/mm). The TV-based detector described previously has been replaced with a gated (30 ns) intensified photodiode array (OSMA IR4-700 from Spectroscopy Instruments) with 700 active channels. A polarization scrambler was placed in front of the spectrometer.

We constructed a new sample cell holder for time-resolved RR spectroscopy at low temperature. The sample was contained in a cylindrical Suprasil cell with 26-mm inner diameter and 6-mm inner height. This cell was placed in a spinning copper block, which was cooled by dry N_2 gas and contained in an insulating housing with a top window for the incoming laser light and a side window for the scattered Raman light. The N_2 gas was cooled by leading it through a copper spiral immersed in a liquid N_2 Dewar vessel. The temperature was monitored with a Chromel–Alumel thermocouple or a Pt-100 resistance sensor placed close to the copper block and was regulated by varying the flow of the N_2 gas. The top and side windows of the housing were flushed from outside with dry N_2 gas to keep away dew. After a predefined temperature was reached in the copper block, the cell was allowed to equilibrate for at least 20 min to reach thermal equilibrium. The temperature of the cell was kept at 183 K for cyclopentane and methanol as solvents, and at 237 K when acetonitrile-d_3 was used.

The chemical composition of the solutions was monitored by gas chromatography (GC; for conditions, see above) before the laser experiments to ensure purity, and after the experiments to follow isomeric conversion during the laser flash photolysis. The conversion between isomers was also followed by evaluating the preresonance Raman spectra of the solutions with respect to vibrational bands from the ground states of different hexatriene isomers.

C. Absorption Measurements. In the time-resolved UV absorption measurements, the sample was irradiated with a pulse from the excimer laser at 308 nm, with a pulse energy of ca. 10 mJ at the sample. The triplet–triplet absorption was measured at right angles to the laser beam with a pulsed Xe lamp, a single-grating monochromator (Jobin Yvon H-20, f = 200 mm) placed after the cell, and a photomultiplier (Hamamatsu 955) coupled to a digital storage oscilloscope (LeCroy 9400). The analyzing wavelength was 318 nm, the spectral bandpass was 8 nm. The absorbance (from sensitizer) at 308 nm was ca. 1 per cm. The laser beam was focused to an area of 2 × 20 mm. The path length of the analyzing light was 20 mm, and the light was masked at the cell to an area of 2 × 4 mm.

The sample was contained in a cylindrical cell with a volume of 5 mL. This cell was placed in a copper block, which was cooled by cold, dry N_2 gas and contained in an insulating housing. The temperature was monitored with a Pt-100 resistance sensor placed in the copper block and was regulated by varying the flow of the N_2 gas. After a predefined temperature in the copper block was reached, the cell was allowed to equilibrate for at least 20 min. Again, the chemical composition of the solution was monitored by GC before and after the experiments. Whereas each Raman spectrum was averaged over many laser pulses, the time-resolved absorption data were obtained with single pulses.

III. Experimental Results

Raman experiments are reported for the following argon-saturated solutions: (1) cyclopentane, 0.817 M acetone, 0.015 M EHT; (2) cyclopentane, 0.817 M acetone, 0.018 M ZHT; (3) methanol, 0.817 M acetone, 0.012 M EHT; (4) cyclopentane, 0.408 M acetone, 0.011 M (*E*)-HT-*3-d*; (5) acetonitrile-d_3, 0.545 M acetone, 0.005 M (*E*)-HT-*3-d*; (6) cyclopentane, 0.408 M acetone, 0.009 M (*E*)-HT-*1,1-d*$_2$; (7) acetonitrile-d_3, 0.545 M acetone, 0.009 M (*E*)-HT-*1,1-d*$_2$. In the time-resolved absorption measurements the solution was (8) methanol, 0.408 M acetone, and 0.018 M EHT.

Subtraction techniques used in the Raman spectra have been discussed in detail previously.[1] Each sample cell was used to obtain spectra by use of (a) the probe laser only, (b) both pump and probe lasers at 60–80-ns time delay between the pump and probe laser pulses, (c) both pump and probe lasers at longer time delay (560–1080 ns), and (d) the probe laser only. Triplet spectra were obtained from spectra b after the subtraction of spectra a and c. Subtraction of spectra a from spectra d allowed the identification of Raman bands arising from stable products of isomerization.

The isomeric conversion was also monitored by GC. For 0.012 M EHT in methanol (solution 3), the amount of *Z* isomer grew from 0.6% to 12% during the experiments. For (*E*)-HT-*3-d*, the amount of *Z* isomer grew from 2% to 10% for the experiments

(4) Langkilde, F. W.; Wilbrandt, R.; Brouwer, A. M. *J. Phys. Chem.* **1990**, *94*, 4809.
(5) Warshel, A.; Karplus, M. *J. Am. Chem. Soc.* **1972**, *94*, 5612.
(6) Warshel, A.; Levitt, M. *QCPE* **1974**, *No. 247*.
(7) Langkilde, F. W.; Wilbrandt, R.; Nielsen, O. F.; Christensen, D. H.; Nicolaisen, F. M. *Spectrochim. Acta* **1987**, *43A*, 1209.

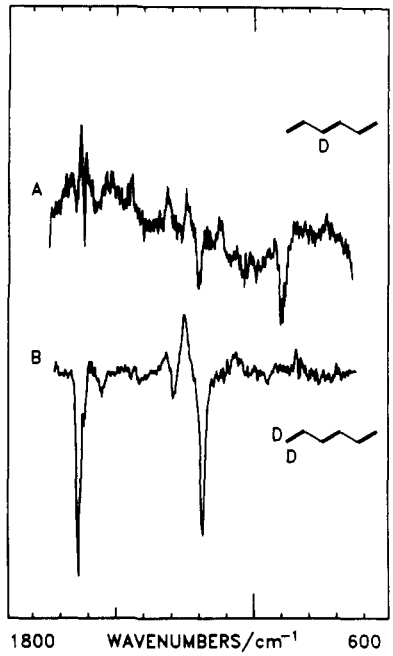

Figure 1. (A) Difference preresonance Raman spectrum excited at 315 nm of 0.011 M (*E*)-HT-*3-d* and 0.408 M acetone in Ar-saturated cyclopentane solution at 183 K after 1200 pump-and-probe pulses. (B) Difference preresonance Raman spectrum excited at 315.75 nm of 0.009 M (*E*)-HT-*1,1-*d_2 and 0.545 M acetone in Ar-saturated acetontrile-d_3 solution at 293 K after 400 pump-and-probe pulses.

with 0.011 M (*E*)-HT-*3-d* in cyclopentane (solution 4), and to 22% for the experiments with 0.005 M (*E*)-HT-*3-d* in acetonitrile-d_3 (solution 5). For (*E*)-HT-*1,1-*d_2, the amount of *Z* isomer grew from 4% to 12% during the experiments with 0.009 M (*E*)-HT-*1,1-*d_2 in cyclopentane (solution 6). In the time-resolved absorption measurements (solution 8), the amount of *Z* isomer grew from 0.6% to 2.1% during the experiments.

A. Ground State. Raman spectra showing the conversion from one ground-state isomer to the other are shown in Figure 1. Subtraction of spectra of type a from spectra of type d is shown in Figure 1A for (*E*)-HT-*3-d* (solution 4), and in Figure 1B for (*E*)-HT-*1,1-*d_2 (solution 7). Similar subtraction spectra are found in ref 2 for (*E*)-HT-*3,4-*d_2 and (*E*)-HT-*2,5-*d_2. The negative bands represent depletion of ground-state *E* isomer, and the positive bands creation of ground-state *Z* isomer, during the laser flash photolysis experiments. As the spectra of the *Z* isomers have not been observed before, we list in Table I the frequencies of the strong preresonance Raman bands of ground-state (*E*)-HT-*3,4-*d_2, (*Z*)-HT-*3,4-*d_2, (*E*)-HT-*3-d*, (*Z*)-HT-*3-d*, (*E*)-HT-*1,1-*d_2, (*Z*)-HT-*1,1-*d_2, (*E*)-HT-*2,5-*d_2, and (*Z*)-HT-*2,5-*d_2. In addition, the spectra in Figure 1 show where one may expect artifacts in the transient triplet spectra reported below, due to changes in the ground-state population of the *E* and *Z* isomers. As shown previously,[1] the *E* and *Z* isomers of 1,3,5-hexatriene yield identical triplet spectra, but the ground-state spectra are different for the two isomers, as seen from Figure 1 and Table I together with previously published spectra.[1,7]

B. Comparison of T_1 RR Spectra of EHT and ZHT at 293 and 183 K. Comparison of spectra obtained at different temperatures is shown in Figures 2 and 3, in order to illustrate the effect of lowering the temperature. Figure 2A shows a probe-only, type a, spectrum of EHT in methanol (solution 3) at 183 K, Figure 2B a pump-and-probe, type b, spectrum at 80-ns delay, and Figure 2C a pump-and-probe, type b, spectrum after subtraction of spectra of types a and c. Parts D–F of Figure 2 show corresponding spectra obtained in methanol at 293 K. The high wavenumber region of spectra 2C and 2F, after rescaling of 2F, is shown in Figure 3. Spectrum 2A (2D) shows ground-state bands from solvent, acetone, and EHT. In spectrum 2B (2E) additional, transient bands appear due to creation of the excited triplet state by the pump laser; the overall intensity is decreased by a factor of 2 due to transient triplet absorption. In spectra 2C (2F) and 3A (3B) the transient triplet bands are seen alone, after subtraction of ground-state bands from solvent and EHT.

The ground-state probe-only spectrum is stronger at 183 K (2A) than at 293 K (2D), in part due to a decrease in bandwidth at lower temperature. The same effect is seen in the pump-and-probe spectrum (2B, 2E), but much more pronounced is the increase at 183 K (2B) in the relative intensity of the additional, transient bands. This effect is found again in the subtraction spectrum of the triplet state (2C, 2F, 3A, 3B) and is reflected in the better signal-to-noise ratio of spectrum 3A compared to 3B. Besides the signal-to-noise ratio and the bandwidths, no significant dif-

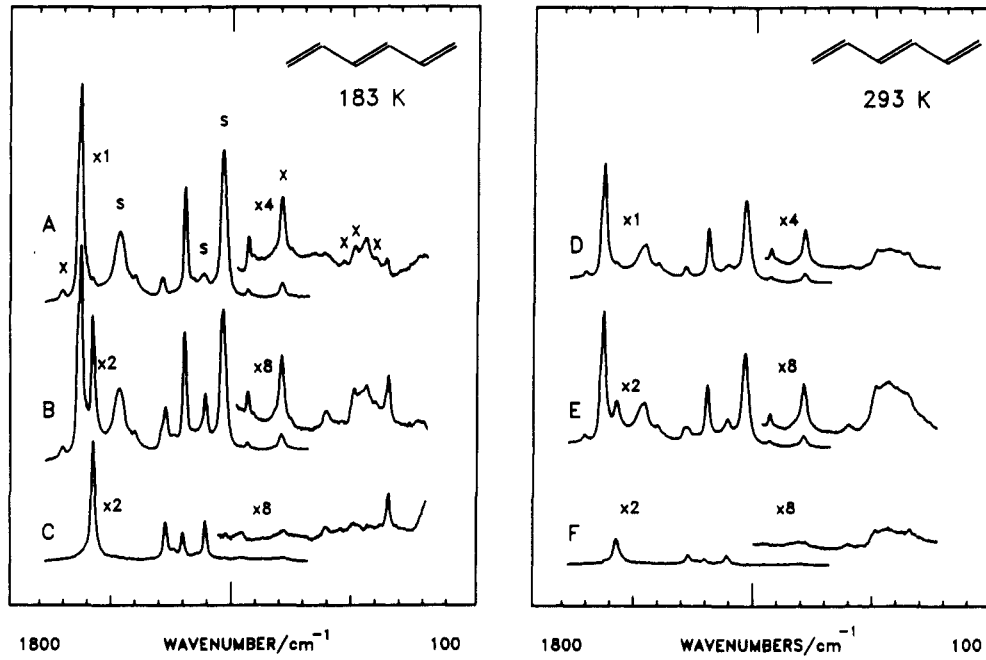

Figure 2. Raman spectra of Ar-saturated solution of 0.012 M EHT in methanol containing 0.817 M acetone. Spectra A–C obtained at 183 K, spectra D–F at 293 K. Spectra A and D, with the probe pulse only; B at a delay of 80 ns and E at a delay of 60 ns between pump-and-probe pulses; C, subtraction from B of A and pump-and-probe spectrum at 1080-ns delay, with appropriate scaling factors; F, subtraction from E of D and pump-and-probe spectrum at 560-ns delay, with appropriate scaling factors. S denotes methanol and X acetone. Pump wavelength 308 nm, probe wavelength 315 nm. Relative scales A–F: 1, 2, 2, 1, 2, 2; all spectra in the region 1000–100 cm^{-1} are scaled up 4 times relative to the spectra in the region 1800–600 cm^{-1}.

TABLE I: Frequencies (cm^{-1}) of Raman Bands of Ground-State (*E*)-HT-*3,4-d*$_2$, (*Z*)-HT-*3,4-d*$_2$, (*E*)-HT-*3-d*, (*Z*)-HT-*3-d*, (*E*)-HT-*1,1-d*$_2$, (*Z*)-HT-*1,1-d*$_2$, (*E*)-HT-*2,5-d*$_2$, and (*Z*)-HT-*2,5-d*$_2$[a]

HT-*3,4-d*$_2$[b]		HT-*3-d*		HT-*1,1-d*$_2$		HT-*2,5-d*$_2$[b]	
E	*Z*	*E*	*Z*	*E*	*Z*	*E*	*Z*
317.5 nm CD_3CN 293 K	317.5 nm CD_3CN 293 K	315 nm C_5H_{10} 183 K	315 nm C_5H_{10} 183 K	315.75 nm CD_3CN 293 K	315.75 nm CD_3CN 293 K	317.5 nm CH_3CN 293 K	317.5 nm CH_3CN 293 K
1610	1320	1201	1314	1285	1317	1618	1252
1563	1132		1243	1185	1251	1570	
1397	897		1123	947	1065	1381	
1290			1063			1295	
1204						1214	
1002						1022	
871							

[a] Excitation wavelength, solvent, and temperature are listed. [b] Reference 2.

TABLE II: Frequency (cm^{-1}) and Intensity of Raman Bands of the Lowest Excited Triplet State of EHT, (*E*)-HT-*3-d*, (*E*)-HT-*1,1-d*$_2$, (*E*)-HT-*3,4-d*$_2$, and (*E*)-HT-*2,5-d*$_2$[a]

EHT		(*E*)-HT-*3-d*		(*E*)-HT-*1,1-d*$_2$	(*E*)-HT-*3,4-d*$_2$[b]	(*E*)-HT-*2,5-d*$_2$[b]
315 nm CH_3OH 183 K	315 nm CH_3OH 293 K	315 nm C_5H_{10} 183 K	315 nm CD_3CN 237 K	315 nm C_5H_{10} 183 K	317.5 nm CD_3CN 293 K	317.5 nm CH_3CN 293 K
1574 s	1571 s	1567 s	1564 s	1573 s	1551 s	1560 s
1334 w	1332 w	1483 w		1442 w	1352 w	1326 w
1271 m	1270 m	1443 m	1444 w	1336 w	1309 m	1286 m
1238 m	1237 w	1320 m	1322 m	1267 s	1209 w	1226 w
1199 m	1200 m	1270 s	1270 s	1229 m	939 m	1140 sh
1140 w	1143 w	1236 w		1221 m	891 m	1123 m
1106 m	1106 m	1202 m	1205 m	1200 m		
957 w	959 w	1152 w	1155 w	1155 m		
778 w	780 w	1129 sh	1127 w	1119 m		
603 w	600 w	1107 m	1104 m	1113 sh		
489 w		1078 m	1078 m	1077 w		
432 w		1025 w	1031 w	986 w		
377 w		985 m	988 m	941 w		
343 m	341 m	927 w	930 w	829 w		
		(882)	890 m	775 w		
		829 w		582 w		
		589 w	592 w	459 w		
		430 w		430 w		
		391 w		381 w		
		338 m	339 m	322 m		

[a] Excitation wavelength, solvent, and temperature are listed. [b] Reference 2.

ferences appear between spectra 3A and 3B.

In order to compare the T_1 RR spectra of EHT and ZHT at low temperature, we recorded the transient triplet spectra of EHT and ZHT in cyclopentane (solutions 1 and 2) in the region 1800–600 cm^{-1} at 183 K. These spectra were identical within experimental limits of error (not shown here).

C. T_1 RR Spectra at 183 K. Time-resolved RR spectra of the lowest triplet state of 1,3,5-hexatriene and deuteriated derivatives obtained by subtraction procedures are shown in Figure 4. Spectrum 4A was obtained from EHT in methanol (solution 3) at 183 K, spectrum 4B from (*E*)-HT-*3-d* in CD_3CN (solution 5) at 237 K, spectrum 4C from (*E*)-HT-*3-d* in cyclopentane (solution 4) at 183 K, and spectrum 4D from (*E*)-HT-*1,1-d*$_2$ in cyclopentane (solution 6) at 183 K. The frequencies of the trplet bands observed in Figure 4 are listed in Table II for EHT, (*E*)-HT-*3-d*, and (*E*)-HT-*1,1-d*$_2$. Previously published values for (*E*)-HT-3,4-d_2 and (*E*)-HT-*2,5-d*$_2$[2] are listed in Table II as well.

In Figure 4A an artifact is observed at 1034 cm^{-1} due to the strong methanol band at this frequency, in parts C and D of Figure 4, artifacts are observed at 886 cm^{-1} due to cyclopentane, and in Figure 4B artifacts are observed at 832 and 348 cm^{-1} due to strong CD_3CN bands. Spectra 4A, 4C, and 4D are shown below in Figures 5–7, respectively, together with the corresponding theoretical spectra.

D. Temperature Dependence of T_1 Lifetime. The decay kinetics of triplet 1,3,5-hexatriene at low temperature was investigated by varying the delay between the pump-and-probe laser pulses. For EHT in cyclopentane (solution 1) at 183 K, we measured the intensity of the strong transient band at 1574 cm^{-1} relative to the

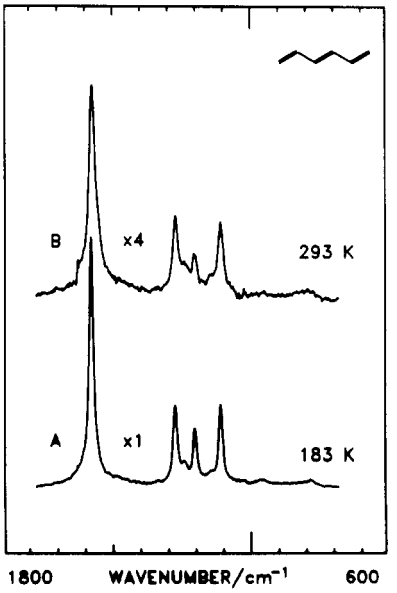

Figure 3. (A) High wavenumber region of spectrum 2C and (B) high wavenumber region of spectrum 2F. Relative scales A, B: 1, 4.

intensity of the solvent bands at 1446 and 1028 cm^{-1} for pump–probe time delays of 80, 150, 250, 350, and 450 ns. For EHT in methanol (solution 3) at 189 K, we measured the intensity of the 1574-cm^{-1} band relative to the intensity of the solvent bands

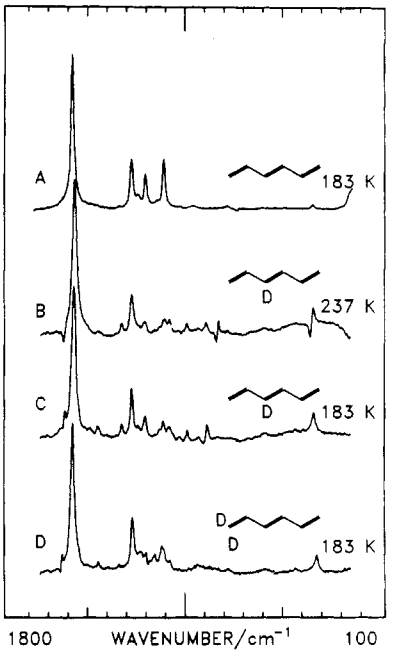

Figure 4. Triplet-state time-resolved resonance Raman spectra of Ar-saturated solutions of (A) methanol, 0.817 M acetone, 0.012 M EHT; (B) acetonitrile-d_3, 0.545 M acetone, 0.005 M (*E*)-HT-*3-d*; (C) cyclopentane, 0.408 M acetone, 0.011 M (*E*)-HT-*3-d*; and (D) cyclopentane, 0.408 M acetone, 0.009 M (*E*)-HT-*1,1-d*$_2$. Solvent, acetone, and hexatriene ground-state bands subtracted. Temperature: A, C, and D 183 K; B 237 K. Pump wavelength 308 nm, probe wavelength 315 nm. Pump–probe delay 80 ns.

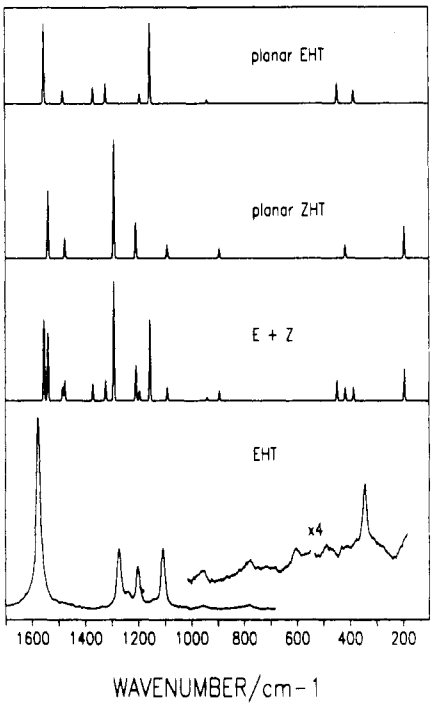

Figure 5. Calculated wavenumbers and relative γ values for the totally symmetric vibrational modes of the *E* form of 1,3,5-hexatriene in resonance with the $T_1 \rightarrow T_5$ transition, the *Z* form ($T_1 \rightarrow T_5$), and the sum of the *E* and *Z* forms, together with the experimental triplet-state time-resolved resonance Raman spectrum obtained at 183 K (same spectrum as Figure 4A).

at 1450 and 1034 cm^{-1} for pump–probe time delays of 60, 110, 210, 310, and 510 ns. Logarithmic plots of the two series of measurements yielded straight lines with first-order rate constants for triplet decay of 4.0×10^6 s^{-1} in cyclopentane (solution 1) and 3.8×10^6 s^{-1} in methanol (solution 3). Previous data for 0.005 M EHT in acetonitrile solution at 293 K[1] yielded a first-order decay rate constant of 10.9×10^6 s^{-1}.

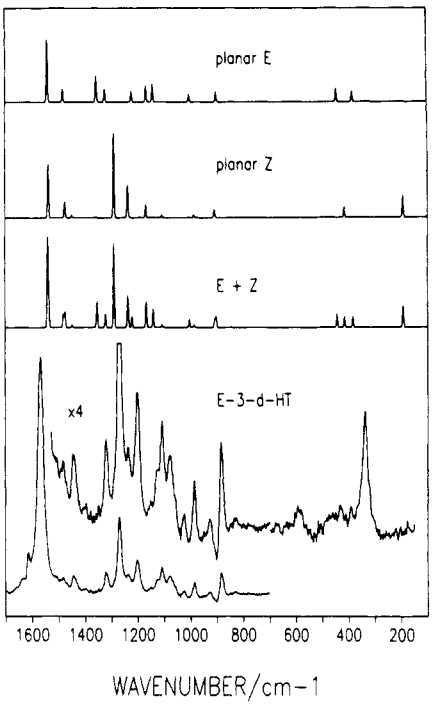

Figure 6. Calculated wavenumbers and relative γ values for the totally symmetric vibrational modes of the *E* form of 3-deuterio-1,3,5-hexatriene in resonance with the $T_1 \rightarrow T_5$ transition, the *Z* form ($T_1 \rightarrow T_5$), and the sum of the *E* and *Z* forms, together with the experimental triplet-state time-resolved resonance Raman spectrum obtained at 183 K (same spectrum as Figure 4C).

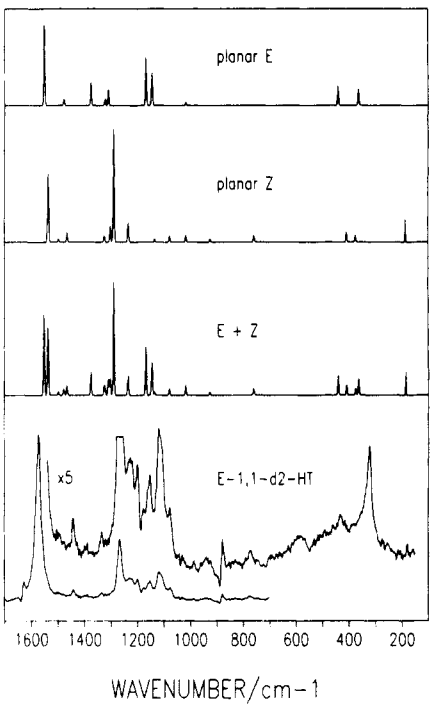

Figure 7. Calculated wavenumbers and relative γ values for the totally symmetric vibrational modes of the *E* form of 1,1-dideuterio-1,3,5-hexatriene in resonance with the $T_1 \rightarrow T_5$ transition, the *Z* form ($T_1 \rightarrow T_5$), and the sum of the *E* and *Z* forms, together with the experimental triplet-state time-resolved resonance Raman spectrum obtained at 183 K (same spectrum as Figure 4D).

Although the decay curves for solutions 1 and 3 were similar, the buildup of T_1 1,3,5-hexatriene by energy transfer from acetone was different for the two solutions. In cyclopentane (solution 1), maximum absorbance was reached before 80 ns, and in methanol (solution 3) between 110 and 210 ns.

Data from time-resolved triplet–triplet absorption measurements at 318 nm of EHT in methanol (solution 8), are shown in Figure

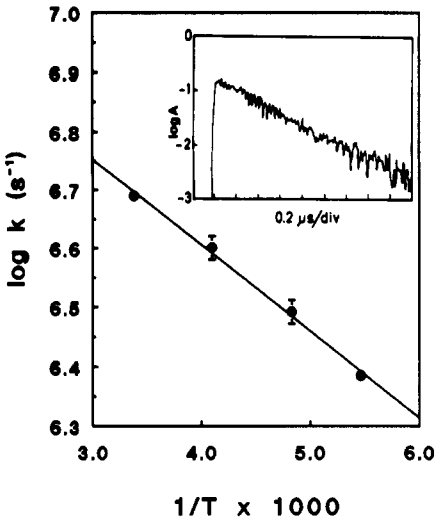

Figure 8. Arrhenius plot of the decay rate constant of T_1 1,3,5-hexatriene for Ar-saturated methanol solution of 0.408 M acetone and 0.018 M EHT. Inset: Logarithm of absorbance for time-resolved triplet–triplet absorption at 183 K, monitored at 318 nm. Pump wavelength 308 nm.

8. At all temperatures, logarithmic plots of triplet–triplet absorption as a function of time yielded straight lines, corresponding to decay rate constants of 4.90×10^6 s^{-1} at 296 K, 3.99×10^6 s^{-1} at 244 K, 3.11×10^6 s^{-1} at 207 K, and 2.43×10^6 s^{-1} at 183 K. The Arrhenius plot in Figure 8 yields an activation energy of 0.7 ± 0.2 kcal/mol and a frequency factor of $(1.6 \pm 0.3) \times 10^7$ s^{-1}. The first-order decay of the triplet–triplet absorption at 183 K is illustrated by the inset in Figure 8. An increase in the buildup time of T_1 1,3,5-hexatriene was clearly observed with decreasing temperature (not shown).

IV. Theoretical Results

A detailed account of the theoretical calculations for HT, HT-*3,4*-d_2, and HT-*2,5*-d_2 has been given previously.[2] Only the most essential results shall be summarized briefly. According to the QCFF/PI calculations, relative minima were found at the planar *E* and planar *Z* geometries of the lowest triplet state of 1,3,5-hexatriene. After geometry optimization, the planar *Z* form was computed at 1.1 kcal/mol above the energy of the planar *E* form, and the geometry perpendicular or twisted (Tw) around the central CC bond at 7.1 kcal/mol above the planar *E* form. Only one strong $T_1 \rightarrow T_n$ (n = 5, 6) transition was computed in the wavelength region of the present experiments for each of the three (*E*, *Z*, and Tw) forms. The $T_1 \rightarrow T_5$ transitions of the *E* and *Z* forms were calculated to be in resonance with the exciting laser wavelength, while that of the Tw form was off-resonance by approximately 1 eV. On the basis of these results and a careful comparison of calculated and experimental T_1 RR spectra, it was concluded that only the planar *E* and *Z* forms contribute to the T_1 RR spectra.

The complete sets of computed wavenumbers and normal modes of the three T_1 forms have been reported previously for HT, HT-*3,4*-d_2, and HT-*2,5*-d_2.[2] Also reported were the Stokes shift parameters γ_i of the totally symmetric vibrational modes in T_1, which are related to geometry changes between T_1 and T_n (n = 5, 6)

$$\gamma_i = (\omega_i/2\hbar)(\Delta Q_i)^2 \quad (1)$$

where ω_i is the vibrational frequency (rad/s), and ΔQ_i is the projection onto the ith normal coordinate of T_1 of the equilibrium geometry change between T_1 and T_n. These parameters are proportional to the Franck–Condon (FC) intensities of totally symmetric modes when the exciting beam is roughly in resonance with the origin of the $T_1 \rightarrow T_n$ transition.

In the present paper, we report the computed wavenumbers and Stokes shift parameters γ_i of the totally symmetric vibrational modes of the lowest triplet state of HT-*3,d* and HT-*1,1*-d_2, together with the previously reported values for HT, in the planar *E* geometry (Table III), in the planar *Z* geometry (Table IV), and in the Tw geometry (Table V). All calculations were performed using the QCFF/PI program as described previously.[2] In Figures 5–7, we have plotted the calculated γ_i values for the planar *E* and planar *Z* forms of HT, HT-*3,d*, and HT-*1,1*-d_2, as a function of frequency together with the experimentally obtained RR spectra in the T_1 state.

Finally, we present in Figure 9 the internal coordinate contribution to the normal modes of 1,3,5-hexatriene in the T_1 state for certain characteristic modes of the planar *E* and *Z* forms.

TABLE III: Computed Wavenumbers (cm^{-1}) and Stokes Shift Parameters γ for the $T_1 \rightarrow T_5$ Transition of Totally Symmetric Normal Modes of (*E*)-1,3,5-Hexatriene, (*E*)-3-Deuterio-1,3,5-hexatriene, and (*E*)-1,1-Dideuterio-1,3,5-hexatriene

EHT		(*E*)-HT-*3,d*		(*E*)-HT-*1,1*-d_2	
ν, cm^{-1}	γ	ν, cm^{-1}	γ	ν, cm^{-1}	γ
1554	0.24	1540	0.24	1552	0.24
1483	0.04	1481	0.05	1478	0.02
1369	0.05	1473	0.00	1428	0.00
1321	0.06	1422	0.00	1376	0.07
1193	0.03	1354	0.10	1323	0.02
1154	0.25	1322	0.05	1310	0.05
939	0.01	1259	0.00	1250	0.00
447	0.06	1221	0.04	1211	0.00
385	0.04	1166	0.06	1168	0.15
		1141	0.07	1145	0.10
		1003	0.03	1017	0.01
		945	0.00	948	0.00
		902	0.04	789	0.00
		582	0.00	570	0.00
		443	0.05	440	0.06
		383	0.04	363	0.05
		176	0.00	169	0.00

TABLE IV: Computed Wavenumbers (cm^{-1}) and Stokes Shift Parameters γ for the $T_1 \rightarrow T_5$ Transition of Totally Symmetric Normal Modes of (*Z*)-1,3,5-Hexatriene, (*Z*)-3-Deuterio-1,3,5-hexatriene, and (*Z*)-1,1-Dideuterio-1,3,5-hexatriene

ZHT		(*Z*)-HT-*3,d*		(*Z*)-HT-*1,1*-d_2	
ν, cm^{-1}	γ	ν, cm^{-1}	γ	ν, cm^{-1}	γ
1539	0.21	1537	0.20	1537	0.21
1475	0.06	1487	0.00	1499	0.01
1331	0.00	1475	0.06	1466	0.03
1290	0.37	1448	0.01	1365	0.00
1207	0.11	1355	0.00	1326	0.02
1089	0.04	1321	0.00	1303	0.05
893	0.03	1290	0.32	1290	0.36
416	0.04	1237	0.12	1235	0.06
194	0.10	1168	0.05	1135	0.01
		1107	0.01	1079	0.02
		985	0.01	1017	0.02
		907	0.03	926	0.01
		859	0.00	760	0.02
		704	0.00	701	0.00
		415	0.04	408	0.03
		398	0.00	374	0.02
		193	0.08	186	0.07

V. Discussion

The spectra shown in Figures 2 and 3 are obtained in methanol, whereas previous experiments were performed in acetonitrile and cyclopentane. The reason for not using acetonitrile in the present work is its relatively high melting point (227 K), and in cyclopentane, due to some yet unknown reason, the room-temperature spectra were of relatively low signal-to-noise ratio.[1,8] As methanol has a low melting point (175 K), and methanol solutions show good T_1 RR spectra at 293 K, this was the solvent chosen for a comparison of spectra obtained at different temperatures. One

(8) Langkilde, F. W.; Jensen, N.-H.; Wilbrandt, R. *Chem. Phys. Lett.* **1985**, *118*, 486.

TABLE V: Computed Wavenumbers (cm^{-1}) and Stokes Shift Parameters γ for the $T_1 \rightarrow T_6$ Transition of Totally Symmetric Normal Modes of 90° Twisted (Tw) 1,3,5-Hexatriene, 3-Deuterio-1,3,5-hexatriene, and 1,1-Dideuterio-1,3,5-hexatriene

HT		HT-*3-d*		HT-*1,1-d*$_2$	
ν, cm^{-1}	γ	ν, cm^{-1}	γ	ν, cm^{-1}	γ
1497	0.00	1491	0.01	1486	0.05
1483	0.09	1480	0.08	1463	0.01
1317	0.12	1314	0.11	1342	0.21
1309	0.15	1309	0.15	1310	0.05
1192	0.00	1296	0.04	1306	0.04
1136	0.00	1231	0.01	1293	0.04
1035	0.00	917	0.04	1025	0.01
919	0.04	895	0.01	938	0.02
821	0.00	681	0.02	773	0.01
731	0.02	407	0.03	736	0.03
582	0.00	362	0.01	644	0.01
411	0.04	358	0.02	401	0.05
367	0.01	-160		362	0.01
140	0.00			340	0.01
-168				-164	

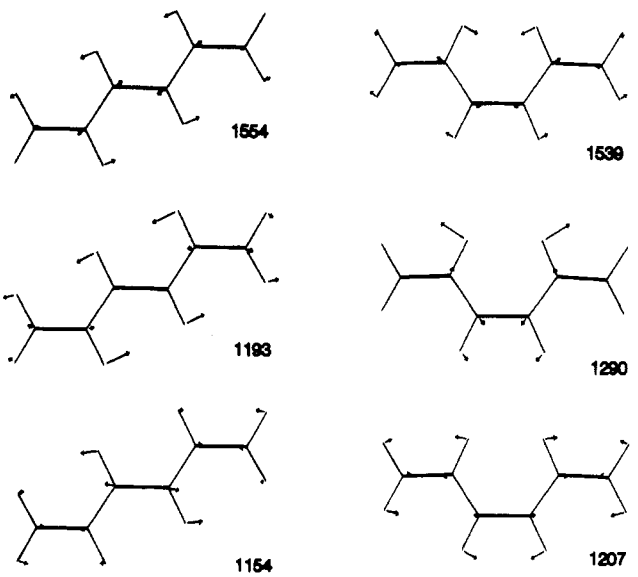

Figure 9. Internal coordinate composition of characteristic normal modes of the planar *E* and *Z* forms of 1,3,5-hexatriene in the T_1 state. Numbers indicate calculated wavenumbers (cm^{-1}).

may then ask whether the short-lived species or mixture of species observed in the T_1 state of 1,3,5-hexatriene at 293 K is the same in different solvents. All bands observed previously in acetonitrile solution are observed in methanol in the present study as well. In addition, a number of hitherto unobserved vibrational bands (at 1332, 959, 780, 600, and 341 cm^{-1}) are found in the present study at 293 K. Of these, a band around 600 cm^{-1} has been noted doubtful in acetonitrile previously, and the newly observed band at 341 cm^{-1} was probably masked by a solvent band (379 cm^{-1} in CH_3CN and 348 cm^{-1} in CD_3CN) in previous studies. All other new bands are weak and have probably been below the noise level in previous experiments. Hence, we conclude that the present T_1 RR spectra obtained at 293 K in methanol are due to the same species as those reported previously in acetonitrile and cyclopentane.

A. Comparison of T_1 RR Spectra of EHT at 293 and 183 K. We now compare the T_1 RR spectra of EHT obtained at 183 and 293 K in methanol (see Figures 2C, 2F, 3A, and 3B, and Table II). The spectra at 293 and 183 K are very similar. The most notable changes, when going to low temperature, are the higher intensity and hence better signal-to-noise ratio, the smaller bandwidth of Raman bands, especially for the 1574-cm^{-1} band, a small shift in wavenumber of particularly the strongest Raman band (from 1571 to 1574 cm^{-1}), and small changes in relative peak intensities. Furthermore, three weak bands (489, 432, and 377 cm^{-1}), which are below the detection limit at 293 K, are observed at 183 K. From this it appears qualitatively that the equilibrium population in T_1, observed at 293 K, is essentially preserved at 183 K, albeit with a somewhat narrower distribution as indicated by the narrowing in Raman bandwidth. These observations shall now be discussed in more detail.

In our previous studies,[1,2] we concluded on the basis of room-temperature spectra that an equilibrium between different forms is established on the T_1 PES within the lifetime of T_1. Two forms, namely, the planar *E* and *Z* forms, were found to contribute to the T_1 RR spectra, while a contribution of the twisted form could not be proved. Furthermore, the calculations suggested that the energies of the relaxed *E* and *Z* forms are similar, and that the resonance scattering conditions (detuning from the 0–0 transition) are approximately the same for the two forms. They can, however, according to the calculations, be distinguished by their different contributions to the RR spectrum of the equilibrium mixture. In particular, the band at 1270 cm^{-1} was attributed to the *Z*, and the band at 1106 cm^{-1} to the *E* form. If this picture is accepted, what is then the effect of lowering the temperature?

The observation of identical T_1 RR spectra at 183 K starting from either the EHT or ZHT ground-state isomer indicates that a full equilibration is attained along the torsional coordinate during the T_1 lifetime. Then, the relative populations of the energy minima at the *E* and *Z* geometries will reflect the energy difference between the two forms, according to a Boltzmann distribution

$$N_1/N_2 = e^{-(E_1-E_2)/k_bT} \quad (2)$$

where k_b is the Boltzmann constant and N_1 and N_2 are the equilibrium populations at the minima 1 (*E*) and 2 (*Z*). If the two forms are isoenergetic, no changes in relative population will occur upon lowering the temperature, whereas the larger their energy difference is, the larger will be the change in the population ratio. Obviously, if the energy difference is large enough (≥3 kcal/mol), the less stable form will be present in a tiny fraction at both temperatures, and hence, only the more stable form will contribute effectively to the observed RR spectrum. Experimentally, the RR spectra of Figure 3 reveal no distinct change in the relative intensities of the 1270- and 1106-cm^{-1} bands, when going from 293 to 183 K.

According to our QCFF/PI calculations,[2] the planar *Z* form is situated at 1.1 kcal/mol above the planar *E* form, corresponding to a ratio of planar *Z* to planar *E* triplet of 0.15 at 293 K and 0.05 at 183 K. Such a change is definitely not observed in the spectra. We estimate that as a lower limit a relative change of 25% would clearly be observable. Assuming that the planar *E* triplet is below planar *Z* in energy, and that the *E*/*Z* ratio at 183 K is ≤1.25 times the ratio at 293 K, eq 2 yields an upper limit of 0.22 kcal/mol for the energy difference between the planar *E* and *Z* forms. This conclusion rests on the band assignment given for the 1270- and 1106-cm^{-1} bands. We shall see below that this assignment is strongly supported by the new results from deuteriated derivatives.

We now turn to the question of the torsional energy barriers on the T_1 PES. Within experimental limits of error, identical T_1 RR spectra are observed for EHT and ZHT at a pump–probe time delay of 80 ns, and no changes in relative intensities of vibrational bands are observed for longer time delays. If the T_1 PES has two minima separated by an energy barrier E_a, the rate constant *k* for the process leading from one minimum to the other can be expressed as

$$k = (k_bT/h)e^{-E_a/k_bT} \quad (3)$$

where k_b is the Boltzmann constant and *h* is Planck's constant. Since at 183 K equilibration between the *E* and *Z* forms is reached in ≤80 ns, E_a must be ≤4.6 kcal/mol. Possibly, friction would further slow down the motion on the T_1 PES and contribute its own activation energy. Thus, it follows that the activation energy derived from eq 3 is a fortiori an upper limit to the T_1 intrinsic intramolecular energy barrier for torsion.

The upper limits of 4.6 kcal/mol for the barrier E_a between the *E* and *Z* forms, and of 0.22 kcal/mol for the energy difference of the *E* and *Z* forms, together indicate a rather flat PES with

TABLE VI: Tentative Assignment of Experimental (Table II) to Calculated[a] Raman Spectra (cm^{-1}) of the Lowest Excited Triplet State of EHT, (*E*)-HT-*3-d*, and (*E*)-HT-*1,1-d*$_2$

EHT		(*E*)-HT-*3-d*		(*E*)-HT-*1,1-d*$_2$	
calc	exp	calc	exp	calc	exp
1554 (*E*), 1539 (*Z*)	1574	1540 (*E*), 1537 (*Z*)	1567	1552 (*E*), 1537 (*Z*)	1573
1483 (*E*)		1481 (*E*)	1483	1499 (*Z*)	
1475 (*Z*)				1478 (*E*)	1442
		1475 (*Z*), 1448 (*Z*)	1443	1466 (*Z*)	
1369 (*E*), 1321 (*E*)	1334			1376 (*E*)	1336
		1354 (*E*), 1322 (*E*)	1320		
1290 (*Z*)	1271			1326 (*Z*)	
1207 (*Z*)	1199			1323 (*E*)	1229
1193 (*E*)	1238	1290 (*Z*)	1270	1310 (*E*)	1221
1154 (*E*)	1106	1237 (*Z*)	1202	1303 (*Z*)	
1089 (*Z*)	1140	1221 (*E*)	1236		
939 (*E*)	957	1168 (*Z*)	1129	1290 (*Z*)	1267
893 (*Z*)	778	1166 (*E*)	1107	1235 (*Z*)	1200
447 (*E*)	432	1141 (*E*)	1078	1168 (*E*)	1155
416 (*Z*)	377	1107 (*Z*)		1145 (*E*)	1119
		1003 (*E*)	985	1135 (*Z*)	1113
385 (*E*) or 194 (*Z*)	343	985 (*Z*)	1025	1079 (*Z*)	1077
		907 (*Z*)	927		
		902 (*E*)	890	1017 (*E*), 1017 (*Z*)	986
		859 (*Z*)	829		
		582 (*E*)	589		
		443 (*E*)	430	926 (*Z*)	941
		415 (*Z*)	391	789 (*E*)	829
				760 (*Z*)	775
		383 (*E*) or 193 (*Z*)	338	570 (*E*)	582
				440 (*E*)	459
				408 (*Z*)	430
				374 (*Z*)	381
				363 (*E*) or 186 (*Z*)	322

[a] *E*, Table III; *Z*, Table IV.

respect to motion along the torsional coordinate of the central CC bond of HT in T_1. This is expected on the basis of the calculated C_3C_4 bond lengths of 1.470 (*E* form) and 1.472 Å (*Z* form) in T_1,[2] which corresponds in length to the ground-state CC single bond (experimental C_2C_3 bond length 1.458 Å for EHT,[9] 1.462 Å for ZHT[10]).

B. Assignment of T_1 RR Spectra at 183 K. Assuming that the planar *E* and planar *Z* forms are present in comparable amounts, we now proceed with a discussion of the assignment of the 183 K triplet RR spectra of EHT, (*E*)-HT-*3-d*, and (*E*)-HT-*1,1-d*$_2$. The spectra in Figure 4 display a large number of bands, and Figure 4 thus constitutes a solid basis for comparison with calculated spectra, as is done in Figures 5–7. We shall now discuss Figures 5–7 to establish more firmly which triplet geometries are present and to assign the observed bands to these geometries. The full assignment between observed and calculated T_1 RR spectra is listed in Table VI for EHT, (*E*)-HT-*3-d*, and (*E*)-HT-*1,1-d*$_2$.

1,3,5-Hexatriene-*d*$_0$. For EHT (Figure 5), we assign the band observed at 1574 cm^{-1} to the ones calculated at 1554 (planar *E*) and 1539 cm^{-1} (planar *Z*), the bands observed at 1271 and 1199 cm^{-1} to the bands calculated at 1290 and 1207 cm^{-1} for planar *Z*, and the band observed at 1106 cm^{-1} to the band calculated at 1154 cm^{-1} for planar *E*.

(*E*)-1,1-Dideuterio-1,3,5-hexatriene. Among Figures 5–7, Figure 7 ((*E*)-HT-*1,1-d*$_2$) gives the clearest evidence for the presence or absence of the different triplet geometries, planar *E*, planar *Z*, and Tw. It is clear that the experimental spectrum in Figure 7 cannot be accounted for by the spectrum calculated for the planar *E* geometry alone. In particular, the intense band observed at 1267 cm^{-1} can be assigned to the strong 1290-cm^{-1} band calculated for planar *Z*, and the observed bands at 941 and 775 cm^{-1} can be assigned to the 926- and 760-cm^{-1} bands calculated for the planar *Z* geometry. The observed 1573-cm^{-1} band then has contributions from both planar *E* and planar *Z*, and the relative intensity of the 1573- and 1267-cm^{-1} bands indicates that planar *E* and planar *Z* are present in comparable amounts.

The following two arguments against the assignment can safely be rejected. (i) A band corresponding to the 186-cm^{-1} band calculated for planar *Z* is not observed. This may be due to the limit of the spectral region observable in the present experiments, which is close to 200 cm^{-1} because of the intense Rayleigh line, or the 186-cm^{-1} band may be calculated at too low a frequency and may correspond to the observed 322-cm^{-1} band. (ii) For both EHT and (*E*)-HT-*1,1-d*$_2$, calculation predicts two strong bands around 1550 cm^{-1}, separated by 15 cm^{-1}, whereas only one strong band is observed for both compounds. This calculated separation of 15 cm^{-1} is small and subject to uncertainty, so it is compatible with the observation of one experimental band. For (*E*)-HT-*2,5-d*$_2$, we calculated two strong bands at 1539 (planar *E* form) and 1512 cm^{-1} (planar *Z* form), and for this compound the FWHM of the observed 1560-cm^{-1} band indeed was larger than for EHT.[2] The band observed around 1550 cm^{-1} is more than twice as strong as the bands observed at lower wavenumbers, in particular the band observed around 1270 cm^{-1}, and in order to explain this observed intensity pattern, we need the bands calculated around 1550 cm^{-1} for both the planar *E* and *Z* forms to account for the intensity of the band observed around 1550 cm^{-1}. Even so, calculation slightly underestimates the intensity of the observed 1550-cm^{-1} band.

For the Tw geometry, the band at 1342 cm^{-1} is by far the most intense calculated one. The 1336-cm^{-1} band is the only one observed close to 1342 cm^{-1}, but it is most likely assigned to the 1376-cm^{-1} band calculated for planar *E*. The strong observed band at 1267 cm^{-1} is assigned to the *Z* form, and in view of its small bandwidth, a contribution from the Tw form seems unlikely. Hence, we conclude that the Tw form at most contributes very weakly to the RR spectrum.

(*E*)-3-Deuterio-1,3,5-hexatriene. Figure 6 ((*E*)-HT-*3-d*) confirms the conclusions reached from the (*E*)-HT-*1,1-d*$_2$ spectrum. To explain the observed spectrum, we need to assume comparable amounts of planar *E* and planar *Z* triplet. With this assignment, the observed 1320-cm^{-1} band corresponds to the 1354-cm^{-1} band calculated for planar *E*, and we do not observe the bands calculated at 1314, 1309, and 1296 cm^{-1} for the Tw geometry.

C. Comparison of Experimental and Calculated T_1 RR Spectra. It should be pointed out that for both Figures 6 and 7, there is a nearly one-to-one correspondence between the observed spectrum and the spectra calculated for the planar *E* and planar *Z* geometries.

When the experimental triplet spectra of EHT, (*E*)-HT-*3-d*, and (*E*)-HT-*1,1-d*$_2$ are viewed together, as in Figure 4, some characteristic bands are nearly unchanged between the three compounds. The HT 1271-cm^{-1} band is found at 1270 cm^{-1} for HT-*3-d* and at 1267 cm^{-1} for HT-*1,1-d*$_2$; this pattern is reproduced by the calculation, where a strong band is calculated at 1290 cm^{-1} for ZHT, (*Z*)-HT-*3-d*, and (*Z*)-HT-*1,1-d*$_2$. The HT 1199-cm^{-1} band is found at 1202 cm^{-1} for HT-*3-d* and at 1200 cm^{-1} for HT-*1,1-d*$_2$; it is calculated at 1207 cm^{-1} for ZHT, at 1237 cm^{-1} for (*Z*)-HT-*3-d*, and at 1235 cm^{-1} for (*Z*)-HT-*1,1-d*$_2$. The HT 1106-cm^{-1} band is found at 1107 cm^{-1} for HT-*3-d* and at 1119 cm^{-1} for HT-*1,1-d*$_2$; it is calculated at 1154 cm^{-1} for EHT, at 1166 cm^{-1} for (*E*)-HT-*3-d*, and at 1145 cm^{-1} for (*E*)-HT-*1,1-d*$_2$. For all these bands, the experimental intensity pattern is reproduced by the calculation.

With the observed band around 1570 cm^{-1} having contributions from both planar *E* and planar *Z* forms, the observed bands around 1270 and 1200 cm^{-1} being due to planar *Z* only, and the observed band around 1110 cm^{-1} being due to planar *E*, we can confirm the relative amounts of planar *E* and planar *Z* triplets. All three spectra, Figure 5 for EHT, Figure 6 for (*E*)-HT-*3-d*, and Figure 7 for (*E*)-HT-*1,1-d*$_2$, indicate that planar *E* and planar *Z* triplets are present in comparable amounts, in good agreement with the energy difference between the two forms below 0.22 kcal/mol,

(9) Trætteberg, M. *Acta Chem. Scand.* **1968**, *22*, 628.
(10) Trætteberg, M. *Acta Chem. Scand.* **1968**, *22*, 2294.

as estimated above. Moreover, mainly on the basis of the less favorable resonance conditions, we believe that a contribution of the Tw form is unlikely. However, to tell whether the Tw form is present or not, additional experiments with a probe laser wavelength around 220 nm ($T_1 \rightarrow T_6$ transition of the Tw form) are necessary.

An important consequence of the above assignment of the triplet spectra is that the strong band observed at 1271 cm^{-1} for nondeuteriated, nonmethylated 1,3,5-hexatriene, and assigned to CH rock coupled to C–C stretch,[2] is indicative of the planar *Z* form. We may thus have a spectral feature that shows whether the planar *Z* form is present in the triplet state, a *Z* band. This rule may be applicable to other polyenes: For the T_1 state of retinal and retinylideneacetaldehydes, Hashimoto et al.[11] assigned a Raman band around 1265 cm^{-1} to the CH bend at a nonmethylated C=C double bond.

Some points should be made with respect to the normal modes shown in Figure 9 for T_1 1,3,5-hexatriene. For EHT, the two strongest T_1 modes, calculated at 1554 and 1154 cm^{-1}, are rotated (Duschinsky effect) with respect to the S_0 modes calculated at 1558 and 1197 cm^{-1} in ref 12. The T_1 1154-cm^{-1} mode has major contributions from C_1C_2, C_3C_4, and C_5C_6 stretches, corresponding to the 1558-cm^{-1} S_0 mode. The T_1 1554-cm^{-1} mode is dominated by C_2C_3 and C_4C_5 stretches, corresponding to the S_0 1197-cm^{-1} mode. For ZHT, a similar rotation of the T_1 1207-cm^{-1} mode is observed with respect to the S_0 1548-cm^{-1} mode. For the T_1 1539-cm^{-1} mode, the rotation is more complicated. The high observed intensity of the modes depicted in Figure 9, in particular of the 1290-cm^{-1} band, is mainly due to their CC stretch components. The phase of the local CC stretches in these normal modes is the same as the phase of the CC bond length changes in the T_1–T_n geometry change, localized mainly in the C_2C_3, C_3C_4, and C_4C_5 bond lengths.[2]

The present triplet Raman spectra of HT-*3-d* and HT-*1,1-*d_2 have a richer vibrational structure than HT because of their lower symmetry. Ground-state (*E*)-1,3,5-hexatriene and also the planar *E* triplet transform according to C_{2h} symmetry and so obey the exclusion principle between Raman and infrared-active vibrations. Deuteriation in the 3-position ((*E*)-HT-*3-d*) lowers the symmetry to C_h and so should lead to a breakdown of the exclusion principle. This is indeed observed when the calculated triplet spectra of EHT and (*E*)-HT-*3-d* are compared, where the EHT bands at 1193 and 1154 cm^{-1} distribute their intensity among the 1221-, 1166-, and 1141-cm^{-1} bands of (*E*)-HT-*3-d*, and the EHT band at 939 cm^{-1} splits into the 1003- and 902-cm^{-1} bands of (*E*)-HT-*3-d*. Most of these bands are dominated by CH (CD) rock. Similar considerations apply to the planar *Z* form, where deuteriation in the 3-position lowers the symmetry from C_{2v} to C_h. For the planar *Z* form, the HT band at 1207 cm^{-1} splits into the 1237- and 1168-cm^{-1} bands of HT-*3-d*, and the HT band at 893 cm^{-1} splits its intensity between the 985- and 907-cm^{-1} bands of HT-*3-d*. For HT-*1,1-*d_2 compared to HT, the EHT band at 1321 cm^{-1} splits into the 1323- and 1310-cm^{-1} bands of (*E*)-HT-*1,1-*d_2, whereas for the planar *Z* form, additional bands appear around 1300, 1100, 1000, 750, and 400 cm^{-1} in the calculated spectra of (*Z*)-HT-*1,1-*d_2.

D. Intensity of T_1 RR Spectra. We shall next address the question of why the triplet Raman spectra are so much stronger at 183 K than at 293 K. From Figures 2 and 3 it is seen that the peak height of the triplet bands is 4 times higher at 183 K and 80-ns delay than at 293 K and 60-ns delay. Several possible explanations exist for this phenomenon:

First, it is seen from Figures 2 and 3 that the triplet Raman bandwidth decreases from 293 to 183 K, so the difference in the integrated band intensities is smaller than the factor 4; this effect is most pronounced for the 1574-cm^{-1} band. Second, due to the longer triplet lifetime at 183 K (see below), the maximum triplet concentration is higher. Third, the triplet–triplet absorption spectrum with a local maximum around 315 nm in toluene at room temperature[13,14] is likely to have a smaller bandwidth at 183 K and a higher extinction coefficient at 315 nm, leading to stronger resonance enhancement of the triplet Raman spectrum. Fourth, the increased Raman intensity at 183 K may be due to a different distribution between triplet geometries. If the planar *E* and *Z* forms alone give rise to RR spectra, and the Tw form is at higher energy than the planar forms, then lowering the temperature should lead to an increase in the relative amount of the planar forms and consequently in the Raman intensities.

In contrast, if the energy of the Tw form were significantly below the energy of the planar forms, the ratio of the planar forms to the Tw form would decrease at lower temperature, leading to weaker triplet Raman spectra. The strong Raman spectra observed at 183 K indicate that the Tw form cannot be much lower in energy than the planar forms. We estimate the upper limit of the E(planar) – E(Tw) energy difference to be 1 kcal/mol. The estimated activation energy E_a of the triplet decay (see below) sets an upper limit for the energy of the Tw form relative to the planar forms of 0.7 kcal/mol.

E. Kinetics of Formation and Decay of the T_1 State. We now turn to the kinetics of the T_1 state. When comparing the kinetics at 293 and 183 K, one has to keep in mind that differences observed may be due to pure temperature effects, but may also be due to changes in viscosity accompanying the temperature changes. Experimental kinetics of formation and decay of EHT in T_1, based on RR observations, were reported above; the first-order decay rate constant was 10.9×10^6 s^{-1} in acetonitrile at 293 K, 4.0×10^6 s^{-1} in cyclopentane at 183 K, and 3.8×10^6 s^{-1} in methanol at 189 K. Data based on time-resolved absorption measurements are shown in Figure 8. It is seen from Figure 8 that the T_1 lifetime increases by a factor of 2 when going from 296 to 183 K. One may then ask whether this is an effect of temperature, viscosity, or both. The viscosity of acetonitrile is 0.369 cP at 290.4 K,[15] that of cyclopentane is ≈3.1 cP at 183 K,[16] and that of methanol is 6.8 cP at 189 K.[17] From the very similar decay rate constants observed in the RR experiments from methanol and cyclopentane, i.e., solutions at similar temperature but considerably different viscosity, it seems most likely that in the present experiments the temperature is the main factor determining the T_1 decay rate. Accepting this view, and assuming an Arrhenius dependence

$$k = Ae^{-E_a/k_bT} \tag{4}$$

the data in Figure 8 yield an activation energy of $E_a = 0.7 \pm 0.2$ kcal/mol and a frequency factor of $A = (1.6 \pm 0.3) \times 10^7$ s^{-1} for the decay of T_1 HT.

The value of the frequency factor does not pertain to the motion on the T_1 PES for which a value of ca. 10^{12} s^{-1} would be expected from eq 3, in agreement with experiments on related systems.[18,19] Rather, it is characteristic of a spin-forbidden, radiationless $T_1 \rightarrow S_0$ intersystem-crossing (ISC) process.[20] The low value of the activation energy suggests that planar and twisted forms are roughly degenerate.

The effect of viscosity, on the other hand, is observable in the slower formation rate of the triplet state in methanol as compared to cyclopentane mentioned above. The formation of T_1 HT occurs by exothermic triplet energy transfer from acetone, i.e., a bimo-

(11) Hashimoto, H.; Mukai, Y.; Koyama, Y. *Chem. Phys. Lett.* **1988**, *152*, 319.
(12) Yoshida, H.; Furukawa, Y.; Tasumi, M. *J. Mol. Struct.* **1989**, *194*, 279.
(13) Gorman, A. A.; Hamblett, I. *Chem. Phys. Lett.* **1983**, *97*, 422.
(14) Langkilde, F. W.; Wilbrandt, R.; Jensen, N.-H. *Chem. Phys. Lett.* **1984**, *111*, 372.
(15) Saltiel, J.; Shannon, P. T.; Zafiriou, O. C.; Uriarte, A. K. *J. Am. Chem. Soc.* **1980**, *102*, 6799.
(16) Yaws, C. L.; Turnbough, A. C. *Chem. Eng. (N.Y.)* **1975**, *82*(26), 119.
(17) *Handbook of Chemistry and Physics*, 57th ed.; CRC Press: Cleveland, OH, 1976–1977 p F-55.
(18) Misawa, H.; Karatsu, T.; Arai, T.; Sakuragi, H.; Tokumaru, K. *Chem. Phys. Lett.* **1988**, *146*, 405.
(19) Karatsu, T.; Tsuchiya, M.; Arai, T.; Sakuragi, H.; Tokumaru, K. *Chem. Phys. Lett.* **1990**, *169*, 36.
(20) Orlandi, G.; Marconi, G. C. *Chem. Phys.* **1975**, *8*, 458.

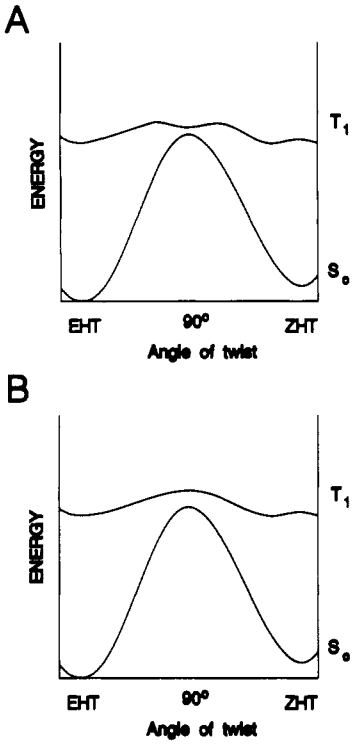

Figure 10. Qualitative potential energy surfaces (PES) of T_1 and S_0 1,3,5-hexatriene for the torsional reaction coordinate of the central CC bond, with (A) and without (B) a local minimum at the 90° twisted geometry.

lecular process, with a nearly diffusion limited rate constant.[15] If it is assumed that triplet energy transfer occurs with a second-order rate constant limited by diffusion, the formation rate of triplet HT can be estimated from the relation $k = (8 \times 10^4 RT/3\eta)$,[15] where k is the bimolecular rate constant and η is the viscosity in poise. Under the present conditions (temperature and molar concentration of HT), this yields formation half-lives of 8 ns in acetonitrile at 293 K, 35 ns in cyclopentane at 183 K, and 94 ns in methanol at 189 K, in good qualitative agreement with the experimental results.

The fact that viscosity differences between cyclopentane at 183 K and methanol at 189 K are expressed in the kinetics of the buildup, but not in the decay of T_1 HT, strongly indicates that the variation of the decay rate constant depends on temperature, not on viscosity.

As mentioned, we monitored by GC the $E \rightarrow Z$ conversion of 1,3,5-hexatriene during the laser flash photolysis experiments at both 293 and 183 K. We found only a slight decrease in the conversion at 183 K. This again qualitatively indicate only a minor influence of viscosity on the decay process under the present experimental conditions.

F. Shape of the T_1 Potential Energy Surface. We shall now attempt to put together the various pieces of information in order to obtain a qualitative picture of the T_1 PES of 1,3,5-hexatriene. The ideas expressed in the following discussion are illustrated in Figure 10. Recent experiments on sensitized photoisomerization of 1,3,5-hexatriene seem to indicate that the ZHT form in T_1 is slightly nonplanar, corresponding to a twist angle greater than 0°;[21] this is taken into account in Figure 10.

Based on the spectroscopic measurements, minima are found on the T_1 PES at planar or nearly planar E and Z geometries. The E and Z forms have very similar energies, the difference being less than 0.22 kcal/mol. These two forms are mainly responsible for the observed RR spectra. A third relative minimum may be present at a centrally twisted geometry. The energy of this Tw form can either be slightly below or, more likely, above the E and Z forms. From comparison of RR spectra at 293 and 183 K, we estimated the Tw form, if below the planar forms, to be at most 1.0 kcal/mol below these. Even if populated to a considerable degree, this Tw form would probably contribute little to the observed RR spectra, due to less favorable resonance conditions.

Torsional equilibration on the T_1 PES occurs much faster than the decay of the triplet population. From the fact that equilibration between the E and Z forms is established at 183 K before 80 ns, we estimated an upper limit of 4.6 kcal/mol for energy barriers between the planar E and Z forms with respect to the torsional coordinate around the central CC bond on the T_1 PES. The Tw form must then also be at most 4.6 kcal/mol above the planar forms. From the dependence of triplet-state lifetime on temperature, we obtained an activation energy of triplet decay of 0.7 kcal/mol. This must also be an upper limit for the energy difference on the T_1 PES between the planar and the twisted forms.

Little is known about the energy gap between the T_1 and S_0 PES. A maximum on the S_0 PES of 1,3,5-hexatriene of 47.5 kcal/mol (46.1 kcal/mol) with respect to the E (Z) form has been calculated at 90° twist around the central CC bond.[22] Experimentally, the activation energy E_a for thermal isomerization of EHT to ZHT has been determined as 43.3 kcal/mol in the gas phase.[23] The vertical triplet energy, obtained from the most intense band of the $S_0 \rightarrow T_1$ absorption spectrum, is 59.4 kcal/mol for EHT and 60.8 kcal/mol for ZHT.[24] The 0–0 energy gap, derived from the first feature of the $S_0 \rightarrow T_1$ absorption spectrum, is 46.9 and 47.7 kcal/mol for EHT and ZHT, respectively.[24] These 0–0 energies are determined with an uncertainty of at least 0.5 kcal/mol. Thus, we can infer only that the relaxed E form has an energy slightly below the energy of the Z form.

For ZHT being 1.4 kcal/mol above EHT in S_0 (theory, ref 22), and the S_0–T_1 0–0 energy gap being 0.8 kcal/mol larger for ZHT than for EHT (experiment, ref 24), the Z form is expected to be 2.2 kcal/mol above the planar E form in T_1. This is in contrast with the present finding of the E and Z forms being within 0.22 kcal/mol in energy in T_1. The reason for this discrepancy is probably that the different methods probe molecules with different degrees of relaxation. Relaxation takes place in T_1 by torsion around the C_3C_4 bond, this being the weakest CC bond in T_1, as reflected in the slight nonplanarity of the Z form, and in particular by changes in CC bond lengths and CCC in-plane bond angles.

There is no distinct measure of the T_1 energy at the Tw geometry. However, the temperature-dependent data presented above suggest that the energy of the Tw form in T_1 lies within 1 kcal/mol from the energy of the E form. Thus, the T_1–S_0 energy gap at 90° is expected to be less than 5 kcal/mol. Although a crossing between the S_0 and T_1 PES in the Tw region cannot be ruled out, it appears unlikely in view of the data presented above.

The T_1 decay at the Tw geometry is much faster than at planar geometries because of the reduced energy gap and the increase of the S_0–T_1 spin–orbit coupling.[20] Model calculations on stilbene[20] showed that, for T_1–S_0 energy gaps smaller than 4 kcal/mol, the decay rate constant at 90° is ca. 10^8 s^{-1}, in substantial agreement with the experimental observation.[25] In contrast, if the $T_1 \rightarrow S_0$ decay were to take place at the planar geometries, the T_1 lifetime would be in the order of 10 ms.[26] For the HT case, the observed triplet lifetimes of 100–300 ns clearly correspond to a decay occurring close to the Tw geometry.

As we have shown above, the temperature dependence of the decay rate of triplet HT can be described by an Arrhenius equation. An attractively simple interpretation of the observed activation energy is that it corresponds to the temperature effect on the equilibrium distribution of planar and twisted forms, the latter being ca. 0.7 kcal/mol higher in energy. The decay rate at the twisted geometry is then the observed frequency factor divided by the population of the twisted form. Alternatively, the temperature effect may be ascribed to the process of reaching a

(21) Møller, S.; Langkilde, F. W.; Wilbrandt, R. *J. Photochem. Photobiol.*, to be published.

(22) Dewar, M. J. S.; Kohn, M. C. *J. Am. Chem. Soc.* **1972**, *94*, 2699.
(23) Orchard, S. W.; Thrush, B. A. *Proc. R. Soc. London* **1974**, *A337*, 257.
(24) Minnaard, N. G.; Havinga, E. *Recl. Trav. Chim. Pays-Bas* **1973**, *92*, 1179.
(25) Görner, H.; Schulte-Frohlinde, D. *J. Phys. Chem.* **1981**, *85*, 1835.
(26) Görner, H.; Schulte-Frohlinde, D. *J. Phys. Chem.* **1979**, *83*, 3107.

critical (not necessarily stationary) point on the PES, ca. 0.7 kcal/mol higher in energy than the planar *E* form, where the T_1–S_0 crossing occurs (see Figure 10B). In this view, the frequency factor simply corresponds to the $T_1 \rightarrow S_0$ ISC rate at the crossing geometry. In either case, a firm conclusion from our work is that the twisted species cannot be much higher in energy than the planar forms.

For the twisted form being 0.7 kcal/mol above the *E* and *Z* forms, the Boltzmann distribution, eq 2, yields a planar/twisted population ratio of 1:0.15 at 183 K, and 1:0.30 at 293 K. With the different resonance conditions, observation of the twisted form in the RR spectra is rather unlikely, as estimated in ref 27.

From the validity of the nonequilibration of excited rotamers (NEER) principle in the T_1 state of 2,5-dimethyl-1,3,5-hexatriene, we have estimated a lower limit of the rotational barrier around the C_2C_3 bond of more than 8 kcal/mol.[3] Most likely, this barrier is similar for 1,3,5-hexatriene, and it is definitely higher than the barrier for the twisting of the central CC bond. This agrees with the computed lengths of the CC bonds in T_1: The optimized length of the C_2C_3 bond is 1.386 Å, while the calculated C_3C_4 bond length is 1.470 Å. Thus, the T_1 PES of EHT for the twisting of the C_2C_3 bond has minima at the tEt (Chart I) and tEc geometries,[27] which are separated by a barrier higher than 8 kcal/mol. Similar considerations apply to the tZt and tZc geometries.

We now want to relate the present picture of the T_1 PES of 1,3,5-hexatriene to recent studies of the T_1 PES of 1,2-diarylethylenes and of arylethylenes.[18,19,28,29] For these compounds, triplet photoisomerization has been divided into adiabatic and diabatic mechanisms. For adiabatic mechanisms, isomerization takes place on the T_1 PES, followed by a vertical decay to the S_0 PES at one of the planar geometries. For diabatic mechanisms, equilibration takes place on the T_1 PES, followed by decay at 90° to the S_0 barrier, from where isomerization proceeds by relaxation to the *E* or *Z* forms. The factors that favor one or the other mechanism have been discussed recently.[30]

In both cases, equilibration takes place on the T_1 PES within the triplet lifetime, and planar geometries are substantially populated. For the diarylethylenes, where the adiabatic mechanism applies, the electronic T_1 state corresponds to an excitation localized on the aromatic moieties. Therefore, the barrier to torsion on the T_1 PES is sufficiently high in these compounds so that the decay takes place predominantly at the planar geometries, and because of an energy gap in the order of 40 kcal/mol, the T_1 lifetime is long (>1 ms). Since decay takes place from a planar T_1 geometry, a planar S_0 minimum is populated, and no further reaction takes place.

In 1,3,5-hexatriene, as well as in stilbene, the T_1 excitation is largely localized on the central C=C double bond. Hence, the T_1 PES has a low barrier or a minimum at 90°. Consequently, although planar geometries are predominant, decay takes place at the Tw geometry, where the T_1–S_0 energy gap is small. However, since at the Tw geometry the S_0 PES has a maximum, the molecules relax to both planar *E* and planar *Z* S_0 geometries, thus giving rise to a diabatic photoisomerization.

Thus, the division of photoreactions into adiabatic and diabatic ones is strictly related to the amount of excitation localized on the central C=C double bond and hence to the size of the chromophores linked to this bond.

VI. Conclusions

In the present paper we have obtained time-resolved RR spectra of the lowest excited triplet state of 1,3,5-hexatriene and its 3-deuterio and 1,1-dideuterio derivatives in solution at 183 K. We have shown that it is possible to obtain spectra under these conditions, and that the quality of the spectra is improved strongly at low temperature.

We have calculated the T_1 RR spectra for the planar *E* and *Z* geometries of the three molecules, and for the geometry that is perpendicular (Tw) at the central CC bond. For each of the three geometries we have identified the strongest $T_1 \rightarrow T_n$ transition and calculated the RR intensities on the basis of geometry changes between T_1 and T_n.

Comparing with the theoretical spectra, we have assigned the observed RR spectra to the planar *E* and planar *Z* geometries, the two geometries being nearly equally populated. For 3-deuterio-1,3,5-hexatriene and 1,1-dideuterio-1,3,5-hexatriene, the assignment between theoretical and experimental spectra is nearly unambiguous, a result which establishes that time-resolved RR spectroscopy in connection with theoretical calculations is a valuable method to determine excited-state molecular structure. In particular, we have shown that a strong triplet Raman band around 1270 cm^{-1} is diagnostic of the planar *Z* geometry.

From comparison of T_1 RR spectra at 293 and 183 K, we have estimated that the *E* and *Z* forms are virtually degenerate, and that the Tw geometry probably is above, and definitely less than 1.0 kcal/mol below, the planar forms. We have measured the triplet–triplet absorption of 1,3,5-hexatriene as a function of temperature; this measurement allows estimation of the frequency factor at ca. 10^7 s^{-1}, a value that agrees with the notion that the rate-determining step of T_1 decay is the $T_1 \rightarrow S_0$ ISC. Viscosity effects are seen at 183 K for the buildup of T_1 1,3,5-hexatriene by energy transfer from a sensitizer, but not for the decay of the T_1 state.

Acknowledgment. This work was supported by the Danish Natural Science Research Council, the Ministero della Pubblica Instruzione of Italy, and a collaborative research grant (Grant 0137/88) from NATO. We thank Dr. K. B. Hansen, Dr. J. Fenger, and M. B. Madsen for support with the experimental facility, and Dr. K. Bajdor and E. Engholm Larsen for construction of the low-temperature cell holder.

Registry No. EHT, 821-07-8; ZHT, 2612-46-6; (*E*)-HT-*3-d*, 135147-57-8; (*E*)-HT-*1,1-d*$_2$, 135147-58-9; (*E*)-HT-*3,4-d*$_2$, 121771-57-1; (*E*)-HT-*2,5-d*$_2$, 121771-58-2; (*Z*)-HT-*3-d*, 135147-59-0; (*Z*)-HT-*1,1-d*$_2$, 135147-60-3; (*Z*)-HT-*3,4-d*$_2$, 128229-83-4; (*Z*)-HT-*2,5-d*$_2$, 135147-61-4.

(27) Negri, F.; Orlandi, G.; Brouwer, A. M.; Langkilde, F. W.; Møller, S.; Wilbrandt, R. *J. Phys. Chem.*, in press.
(28) Arai, T.; Karatsu, T.; Sakuragi, H.; Tokumaru, K. *Tetrahedron Lett.* **1983**, *24*, 2873.
(29) Arai, T.; Karatsu, T.; Misawa, H.; Kuriyama, Y.; Okamoto, H.; Hiresaki, T.; Furuuchi, H.; Zeng, H.; Sakuragi, H.; Tokumaru, K. *Pure Appl. Chem.* **1988**, *60*, 989.
(30) Orlandi, G.; Negri, F.; Mazzucato, U.; Bartocci, G. *J. Photochem. Photobiol.*, in press.